

NIST Technical Note 2079

Theoretical Basis of the Direct-Comparison System for Power Calibration Including Equivalent Source Mismatch

Jeffrey A. Jargon
Dazhen Gu
Christian J. Long
Aaron M. Hagerstrom
Angela C. Stelson
Ann F. Monke

This publication is available free of charge from:
<https://doi.org/10.6028/NIST.TN.2079>

NIST
**National Institute of
Standards and Technology**
U.S. Department of Commerce

NIST Technical Note 2079

Theoretical Basis of the Direct-Comparison System for Power Calibration Including Equivalent Source Mismatch

Jeffrey A. Jargon
Dazhen Gu
Christian J. Long
Aaron M. Hagerstrom
Angela C. Stelson
Ann F. Monke
*RF Technology Division
Communications Technology Laboratory*

This publication is available free of charge from:
<https://doi.org/10.6028/NIST.TN.2079>

December 2019



U.S. Department of Commerce
Wilbur L. Ross, Jr., Secretary

National Institute of Standards and Technology
Walter Copan, NIST Director and Undersecretary of Commerce for Standards and Technology

Certain commercial entities, equipment, or materials may be identified in this document in order to describe an experimental procedure or concept adequately. Such identification is not intended to imply recommendation or endorsement by the National Institute of Standards and Technology, nor is it intended to imply that the entities, materials, or equipment are necessarily the best available for the purpose.

National Institute of Standards and Technology Technical Note 2079
Natl. Inst. Stand. Technol. Tech. Note 2079, 25 pages (December 2019)
CODEN: NTNOEF

This publication is available free of charge from:
<https://doi.org/10.6028/NIST.TN.2079>

Abstract

In this report, we provide derivations for two equations that serve as the basis for the direct-comparison system, a transfer apparatus for comparing microwave power sensors. The system consists of a synthesizer that provides a signal to the input of a power divider. A monitor power sensor is connected to one of the divider's output ports. During the first portion of the measurement, a transfer standard is connected to the other output port of the divider, and the indicated powers of the transfer standard and monitor are measured. Next, the transfer standard is replaced with an unknown power sensor to be calibrated, and the indicated powers of the unknown device and monitor are measured. Utilizing rules governing flow-diagrams for scattering-parameters and definitions of delivered power, we derive the effective efficiency of an unknown power sensor as a function of the transfer standard's effective efficiency in conjunction with power readings of both sensors and a monitor sensor, as well as reflection coefficients of the sensors and the equivalent source reflection coefficient of the power divider. Our derivation provides the definition of the equivalent source reflection coefficient. We also derive a correction term for the case when an adapter is connected to the transfer standard. Finally, we review the most widely-accepted approach for determining the equivalent source reflection coefficient of a three-port device, such as a power divider, and provide simplistic and comprehensive derivations that demonstrate its independence of the external impedances at two of its ports.

Key words

Calibration; derivation; direct-comparison system; equivalent source mismatch; power.

Table of Contents

1. Introduction	1
2. Direct Comparison System	2
2.1. Adapter Correction	5
3. Equivalent Source Mismatch.....	8
3.1. One-Port Error Model	8
3.2. Simplistic Derivation.....	11
3.3. Comprehensive Derivation.....	13
4. Conclusions.....	17
References	17

List of Variables

Variable	Definition
a_i, b_i	Complex, frequency-domain waves at port i
a_S	Complex, frequency domain wave emanating from the source
e_{00}	Directivity error term of one-port VNA
e_{11}	Port match error term of one-port VNA
$e_{10}e_{01}$	Tracking error term of one-port VNA
P_D	Delivered power
P_I	Incident power
P_{MS}	Measured dc-substituted power of monitor sensor with the transfer standard connected
P_{MU}	Measured dc-substituted power of monitor sensor with the unknown sensor connected
S_{ij}	Scattering-parameter from port j to port i
Γ_G	Equivalent source mismatch of a three-port device
Γ_M	Reflection coefficient of the monitor sensor
Γ_S	Reflection coefficient of the transfer standard
Γ_U	Reflection coefficient of the unknown sensor
Γ'	Measured reflection coefficient
η_M	Effective efficiency of the monitor sensor
η_S	Effective efficiency of the transfer standard
$\eta's$	Effective efficiency of the transfer standard with an adapter connected
η_U	Effective efficiency of the unknown sensor

1. Introduction

The National Institute of Standards and Technology (NIST) offers calibration services for microwave power sensors and provides measurements of effective efficiency and calibration factor for thermistor, thermoelectric, and thin-film sensors. In the coaxial environment, measurements are implemented for GPC-7, Type-N, 3.5 mm, 2.92 mm, and 2.4 mm connectors for frequencies between 100 kHz and 50 GHz.

Although bolometric power sensors characterized by use of calorimeters serve as primary, traceable power standards [1], it is impractical to measure most sensors this way due to high costs, time constraints, and incompatible sensor designs. Most sensors are either not bolometric or do not have thermal properties required for measurements in a calorimeter. Thus, most coaxial power calibrations are performed using a direct-comparison approach, in which a test sensor is compared with a bolometric transfer standard that has previously been characterized by use of a calorimeter [2]. The advantage of this method is that it is based upon commercially-available, wide-band resistive power dividers, or alternatively directional couplers in waveguide environments. The disadvantage is that mismatch corrections must be accounted for, so reflection coefficients of every device must be measured by use of a calibrated vector network analyzer (VNA).

A simplified schematic of a direct-comparison system is shown in Fig. 1. A synthesizer provides a continuous wave (CW) signal to the input port (port 1) of a power divider. A monitor power sensor is connected to one of the divider's output ports (port 3 in this example). During the first portion of the measurement, a transfer standard is connected to the other output port of the divider (port 2 in this example), and the indicated powers of the transfer standard P_S and monitor P_M are measured as functions of frequency. Next, the transfer standard is replaced with an unknown power sensor to be calibrated, and the indicated powers of the unknown device P_U and monitor P_M are measured.

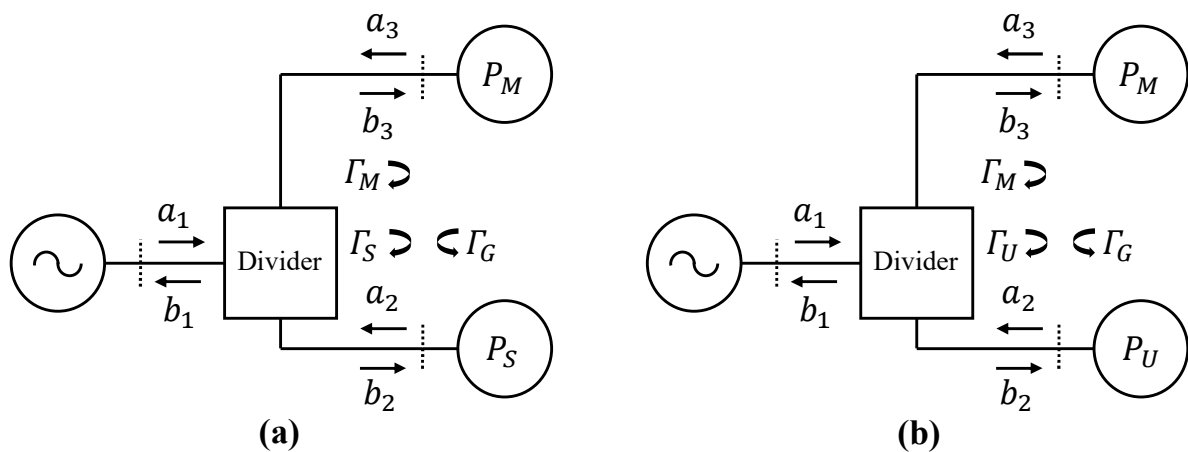


Fig. 1. Simplified schematic diagram of a direct-comparison system for power calibration: (a) with transfer standard connected to port 2, and (b) with unknown sensor connected to port 2.

The effective efficiency of the unknown power sensor η_U can be determined by use of the following equation [3]:

$$\eta_U = \eta_S \frac{P_{MS} P_U (1 - |\Gamma_S|^2) |1 - \Gamma_G \Gamma_U|^2}{P_{MU} P_S (1 - |\Gamma_U|^2) |1 - \Gamma_G \Gamma_S|^2}, \quad (1.1)$$

where the effective efficiency of the transfer standard η_S is determined by use of a calorimeter. The reflection coefficients of the transfer standard Γ_S , unknown device Γ_U , and monitor sensor Γ_M are determined by use of a one-port measurement with a calibrated vector network analyzer (VNA) [4], and P_{MS} and P_{MU} are the measured dc substituted powers of the monitor sensor with the transfer standard and unknown sensor connected, respectively. The equivalent source mismatch Γ_G is defined in terms of the following calibrated S -parameters of the divider:

$$\Gamma_G \stackrel{\text{def}}{=} S_{22} - \frac{S_{21} S_{32}}{S_{31}}, \quad (1.2)$$

and is measured using the technique presented in [5]. It turns out this term is a byproduct of the derivation of Eq. (1.1), as will be shown in the following section.

In this document, we provide derivations for Eq. (1.1) and Eq. (1.2), which serve as the basis for the direct-comparison system. In Sec. 2, we derive these two equations, as well as a correction term for the case when an adapter is connected to the transfer standard. In Sec. 3, we review the most widely-accepted approach for determining the equivalent source reflection coefficient of a three-port device, such as a power divider, and provide simplistic and comprehensive derivations that demonstrate its independence of the external impedances at two of its ports.

2. Direct Comparison System

In this section, we derive the two main equations governing the direct-comparison system for power calibration (Eq. (1.1) and Eq. (1.2)). We begin with the scattering-matrix representation of a three-port device [6], which represents the divider:

$$\begin{bmatrix} b_1 \\ b_2 \\ b_3 \end{bmatrix} = \begin{bmatrix} S_{11} & S_{12} & S_{13} \\ S_{21} & S_{22} & S_{23} \\ S_{31} & S_{32} & S_{33} \end{bmatrix} \begin{bmatrix} a_1 \\ a_2 \\ a_3 \end{bmatrix}. \quad (2.1)$$

Here, a_i and b_i refer to complex, frequency-domain forward and backward waves normalized to a 50Ω reference impedance, and S_{ij} represent the scattering-parameters (S -parameters) relating the input at port j to the output at port i . From Eq. (2.1), we can extract the equations for waves b_2 and b_3 :

$$b_2 = S_{21} a_1 + S_{22} a_2 + S_{23} a_3 \quad (2.2)$$

and

$$b_3 = S_{31}a_1 + S_{32}a_2 + S_{33}a_3. \quad (2.3)$$

When the transfer standard is connected to port 2 of the divider, as shown in Fig. 1, the waves at port 2 are related by

$$a_2 = \Gamma_S b_2, \quad (2.4)$$

where Γ_S is the reflection coefficient of the transfer standard. Likewise, the waves at port 3 are related by

$$a_3 = \Gamma_M b_3, \quad (2.5)$$

where Γ_M is the reflection coefficient of the monitor sensor. Substituting Eq. (2.4) and Eq. (2.5) into Eq. (2.2) and Eq. (2.3) gives

$$b_2 = S_{21}a_1 + S_{22}\Gamma_S b_2 + S_{23}\Gamma_M b_3 \quad (2.6)$$

and

$$b_3 = S_{31}a_1 + S_{32}\Gamma_S b_2 + S_{33}\Gamma_M b_3. \quad (2.7)$$

Solving Eq. (2.6) and Eq. (2.7) in terms of a_1 results in

$$a_1 = \frac{1}{S_{21}}(b_2 - S_{22}\Gamma_S b_2 - S_{23}\Gamma_M b_3) \quad (2.8)$$

and

$$a_1 = \frac{1}{S_{31}}(b_3 - S_{32}\Gamma_S b_2 - S_{33}\Gamma_M b_3). \quad (2.9)$$

Equating Eq. (2.8) and Eq. (2.9) gives

$$S_{31}(b_2 - S_{22}\Gamma_S b_2 - S_{23}\Gamma_M b_3) = S_{21}(b_3 - S_{32}\Gamma_S b_2 - S_{33}\Gamma_M b_3) \quad (2.10)$$

or alternatively in terms of b_2 and b_3

$$b_2(S_{31} - S_{22}S_{31}\Gamma_S + S_{21}S_{32}\Gamma_S) = b_3(S_{21} - S_{21}S_{33}\Gamma_M + S_{31}S_{23}\Gamma_M). \quad (2.11)$$

Solving for the ratio of b_2 over b_3 gives

$$\frac{b_2}{b_3} = \frac{S_{21} - S_{21}S_{33}\Gamma_M + S_{31}S_{23}\Gamma_M}{S_{31} - S_{22}S_{31}\Gamma_S + S_{21}S_{32}\Gamma_S}. \quad (2.12)$$

The power delivered to the transfer standard at port 2, P_{D2} , is given by [7]

$$P_{D2} = |b_2|^2 - |a_2|^2 = |b_2|^2(1 - |\Gamma_S|^2), \quad (2.13)$$

and the power delivered to the monitor sensor at port 3, P_{D3} , is given by

$$P_{D3} = |b_3|^2 - |a_3|^2 = |b_3|^2(1 - |\Gamma_M|^2). \quad (2.14)$$

Thus, the ratio of Eq. (2.13) and Eq. (2.14) is

$$\frac{P_{D2}}{P_{D3}} = \frac{|b_2|^2 (1 - |\Gamma_S|^2)}{|b_3|^2 (1 - |\Gamma_M|^2)}. \quad (2.15)$$

Substituting Eq. (2.12) into Eq. (2.15) gives

$$\frac{P_{D2}}{P_{D3}} = \frac{|S_{21} - S_{21}S_{33}\Gamma_M + S_{31}S_{23}\Gamma_M|^2 (1 - |\Gamma_S|^2)}{|S_{31} - S_{22}S_{31}\Gamma_S + S_{21}S_{32}\Gamma_S|^2 (1 - |\Gamma_M|^2)}. \quad (2.16)$$

The effective efficiency η of a power sensor is defined as the ratio of the substituted power, determined by the electronics of the power meter, over the delivered power. Thus, the effective efficiency of the transfer standard η_S is

$$\eta_S = P_S/P_{D2}, \quad (2.17)$$

where P_S is the dc substituted power of the transfer standard [8]. Solving for the delivered power gives

$$P_{D2} = P_S/\eta_S. \quad (2.18)$$

Likewise, the effective efficiency of the monitor sensor η_M is

$$\eta_M = P_{MS}/P_{D3}, \quad (2.19)$$

where P_{MS} is the dc substituted power of the monitor sensor when the transfer standard is connected to port 2. Solving for the delivered power gives

$$P_{D3} = P_{MS}/\eta_M. \quad (2.20)$$

Substituting Eq. (2.18) and Eq. (2.20) into Eq. (2.16) gives

$$\frac{P_S/\eta_S}{P_{MS}/\eta_M} = \frac{|S_{21} - S_{21}S_{33}\Gamma_M + S_{31}S_{23}\Gamma_M|^2 (1 - |\Gamma_S|^2)}{|S_{31} - S_{22}S_{31}\Gamma_S + S_{21}S_{32}\Gamma_S|^2 (1 - |\Gamma_M|^2)}. \quad (2.21)$$

A similar equation may be obtained when the unknown device is connected to port 2:

$$\frac{P_U/\eta_U}{P_{MU}/\eta_M} = \frac{|S_{21} - S_{21}S_{33}\Gamma_M + S_{31}S_{23}\Gamma_M|^2 (1 - |\Gamma_U|^2)}{|S_{31} - S_{22}S_{31}\Gamma_U + S_{21}S_{32}\Gamma_U|^2 (1 - |\Gamma_M|^2)}, \quad (2.22)$$

where P_U is the dc substituted power of the unknown device, P_{MU} is the dc substituted power of the monitor sensor when the unknown device is connected to port 2, η_U is the effective efficiency of the unknown device, and Γ_U is the reflection coefficient of the unknown device.

The ratio of Eq. (2.21) to Eq. (2.22) is

$$\frac{(P_S/\eta_S)(P_{MU}/\eta_M)}{(P_{MS}/\eta_M)(P_U/\eta_U)} = \frac{|S_{31} - S_{22}S_{31}\Gamma_U + S_{21}S_{32}\Gamma_U|^2 (1 - |\Gamma_S|^2)}{|S_{31} - S_{22}S_{31}\Gamma_S + S_{21}S_{32}\Gamma_S|^2 (1 - |\Gamma_U|^2)}. \quad (2.23)$$

Solving for the effective efficiency of the unknown device gives

$$\eta_U = \eta_S \frac{P_{MS} P_U (1 - |\Gamma_S|^2) |1 - (S_{22} - S_{21}S_{32}/S_{31})\Gamma_U|^2}{P_{MU} P_S (1 - |\Gamma_U|^2) |1 - (S_{22} - S_{21}S_{32}/S_{31})\Gamma_S|^2}, \quad (2.24)$$

where Γ_G may be defined as [9]

$$\Gamma_G \stackrel{\text{def}}{=} S_{22} - \frac{S_{21}S_{32}}{S_{31}}. \quad (2.25)$$

This term is commonly referred to as the equivalent source mismatch [10]. Equation Eq. (2.24) can then be rewritten as

$$\eta_U = \eta_S \frac{P_{MS} P_U (1 - |\Gamma_S|^2) |1 - \Gamma_G \Gamma_U|^2}{P_{MU} P_S (1 - |\Gamma_U|^2) |1 - \Gamma_G \Gamma_S|^2}. \quad (2.26)$$

Equations Eq. (2.25) and Eq. (2.26) provide the basis of the direct-comparison system for power calibration.

2.1. Adapter Correction

Oftentimes, during the calibration of a power sensor, an adapter is required to make a connection between the transfer standard and the divider [11, 12], as illustrated in Fig. 2. This requires corrections be made to the reflection coefficient Γ_S and effective efficiency η_S to account for the S -parameters of the adapter. In this subsection, we derive equations for the corrected values, Γ'_S and η'_S . The waves at port 1 of the adapter are related by

$$b_1 = \Gamma'_S a_1. \quad (2.27)$$

Next, solving for b_1 and b_2 , illustrated in the flow diagram of Fig. 2, gives

$$b_1 = S_{11}^A a_1 + S_{12}^A a_2 \quad (2.28)$$

and

$$b_2 = S_{21}^A a_1 + S_{22}^A a_2. \quad (2.29)$$

The waves at port 2 of the adapter are related by

$$a_2 = \Gamma_S b_2. \quad (2.30)$$

Substituting Eq. (2.30) into Eq. (2.29) gives

$$a_2/\Gamma_S = S_{21}^A a_1 + S_{22}^A a_2 \quad (2.31)$$

or

$$a_2 = \frac{S_{21}^A \Gamma_S a_1}{1 - S_{22}^A \Gamma_S} \quad (2.32)$$

Substituting Eq. (2.32) into Eq. (2.28) gives

$$b_1 = S_{11}^A a_1 + \frac{S_{12}^A S_{21}^A \Gamma_S a_1}{1 - S_{22}^A \Gamma_S}. \quad (2.33)$$

Dividing both sides of Eq. (2.33) by a_1 and substituting the result into Eq. (2.27) gives the corrected value of Γ'_S , the reflection coefficient of the adapter terminated with the transfer standard:

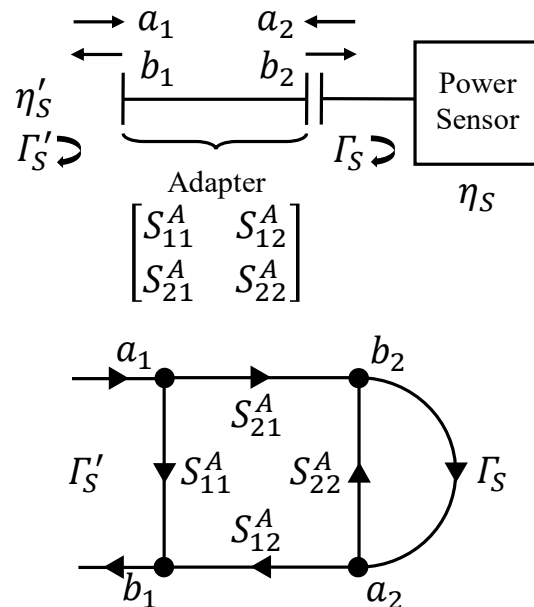


Fig. 2. The upper portion depicts an adapter connected to the transfer standard, and the lower portion depicts the flow diagram including reflection coefficients and S -parameters of the adapter.

$$\Gamma'_S = S_{11}^A + \frac{S_{12}^A S_{21}^A \Gamma_S}{1 - S_{22}^A \Gamma_S}. \quad (2.34)$$

Next, we solve for the corrected value of η'_S , the effective efficiency of the adapter terminated with the transfer standard. We begin by substituting Eq. (2.30) into Eq. (2.29) and solving for b_2 , which gives

$$b_2 = \frac{S_{21}^A}{1 - S_{22}^A \Gamma_S} a_1 \quad (2.35)$$

The power incident on the adapter at port 1, P'_I , is given by [7]

$$P'_I = |a_1|^2. \quad (2.36)$$

The power delivered to the adapter at port 1, P'_D , is given by

$$P'_D = P'_I(1 - |\Gamma'_S|^2) = |a_1|^2(1 - |\Gamma'_S|^2). \quad (2.37)$$

The power incident on the transfer standard at port 2, P_I , is given by

$$P_I = |b_2|^2. \quad (2.38)$$

Substituting Eq. (2.35) into Eq. (2.38) gives

$$P_I = \frac{|S_{21}^A|^2 |a_1|^2}{|1 - S_{22}^A \Gamma_S|^2}. \quad (2.39)$$

The power delivered to the transfer standard at port 2, P_D , is given by

$$P_D = P_I(1 - |\Gamma_S|^2) = \frac{|S_{21}^A|^2 |a_1|^2}{|1 - S_{22}^A \Gamma_S|^2} (1 - |\Gamma_S|^2). \quad (2.40)$$

As mentioned in Sec. 2, the effective efficiency of a power sensor is defined as the ratio of the substituted power over the delivered power. Thus, the effective efficiency of the transfer standard at port 2, denoted as η_S , is given by

$$\eta_S = \frac{P_{DC}}{P_D}, \quad (2.41)$$

and the effective efficiency at port 1, denoted as η'_S , is given by

$$\eta'_S = \frac{P_{DC}}{P'_D}. \quad (2.42)$$

Solving Eq. (2.41) and Eq. (2.42) for P_{DC} and equating them gives

$$\eta'_s P'_D = \eta_s P_D. \quad (2.43)$$

Solving Eq. (2.43) for η'_s gives

$$\eta'_s = \eta_s \frac{P_D}{P'_D}. \quad (2.44)$$

Substituting Eq. (2.37) and Eq. (2.40) into Eq. (2.44) allows us to solve for the corrected value of η'_s , the effective efficiency of the adapter terminated with the transfer standard as a function of η_s , Γ_S , Γ'_S , and the S -parameters of the adapter:

$$\eta'_s = \eta_s \frac{1 - |\Gamma_S|^2}{1 - |\Gamma'_S|^2} \frac{|S_{21}^A|^2}{|1 - S_{22}^A \Gamma_S|^2}. \quad (2.45)$$

Equation (2.45) is identical to that presented in [12].

An alternative formulation, which has been historically used internally at NIST, can be written as the effective efficiency of the transfer standard η_s as a function of η'_s , Γ_S , and the S -parameters of the adapter. This may be accomplished by substituting Eq. (2.34) into Eq. (2.45) and solving for η_s , which gives

$$\eta_s = \eta'_s \frac{[|1 - S_{22}^A \Gamma_S|^2 - |(S_{12}^A S_{21}^A - S_{11}^A S_{22}^A) \Gamma_S + S_{11}^A|^2]}{|S_{21}^A|^2 (1 - |\Gamma_S|^2)}. \quad (2.46)$$

In this section, we have derived the two equations, Eq. (2.25) and Eq. (2.26), that serve as the basis for the direct-comparison system, as well as a correction term, alternatively Eq. (2.45) or Eq. (2.46), for the case when an adapter is connected to the transfer standard.

3. Equivalent Source Mismatch

From Eq. (2.25), we can see that the equivalent source mismatch is exclusively a function of the S -parameters of the power divider and invariant of the signal generator and power sensors connected to it. Although various techniques have been developed to determine this quantity, the most widely-accepted approach is the method developed by Juroshek [5], which makes use of a one-port VNA calibration.

In Sec. 3.1, we review this method. Then, in the following sections, we provide simplistic and comprehensive derivations.

3.1. One-Port Error Model

The upper portion of Fig. 3 illustrates a simplified diagram of a one-port VNA, which consists of a signal generator, two directional couplers connected back-to-back, and an unknown one-port device. Since the measurement system is not perfect, the reflection coefficient measured by the VNA must be corrected with a calibration. Imperfections in the VNA are modeled by taking the linear errors and combining them into a two-port error box between the couplers and

the unknown one-port device. Since ratio measurements are taken, only three terms are required. The lower portion of Fig. 3 shows the flow graph of the two-port error box connected to the unknown reflection coefficient. The measured reflection coefficient, Γ' , is mathematically related to the actual reflection coefficient, Γ , by three error terms: directivity e_{00} , port match e_{11} , and tracking $e_{10}e_{01}$. These three terms can be determined with measurements of three known calibrations artifacts such as an open, short, and load.

Solving the one-port flow graph in Fig. 3 results in a bilinear relationship between the measured reflection coefficient

$$\Gamma' = b_0/a_0 \tag{3.1}$$

and the actual reflection coefficient

$$\Gamma = \frac{a_1}{b_1} = \frac{(b_0/a_0) - e_{00}}{(b_0/a_0)e_{11} - \Delta_e} = \frac{\Gamma' - e_{00}}{\Gamma'e_{11} - \Delta_e}, \tag{3.2}$$

where

$$\Delta_e = e_{00}e_{11} - e_{10}e_{01}. \tag{3.3}$$

For the one-port VNA, e_{11} is analogous to Γ_G of the incident coupler (measuring a_0).

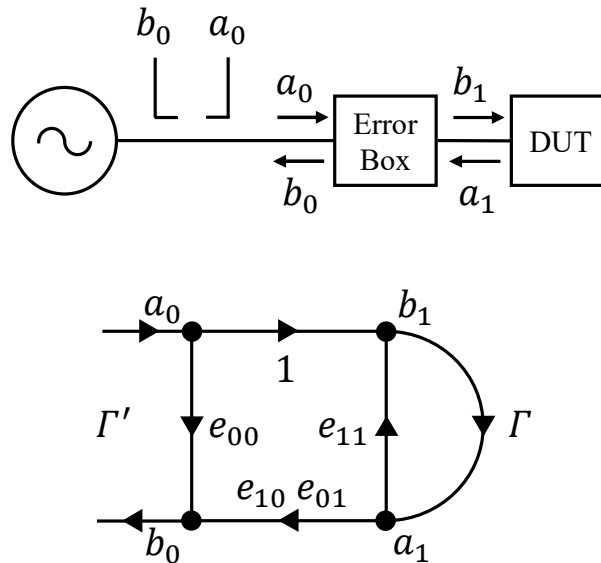


Fig. 3. The upper portion depicts a simplified diagram of a port VNA, and the lower portion depicts the flow diagram including the two-port error box that relates the measured reflection coefficient, Γ' , to the actual reflection coefficient, Γ .

Similarly, the scattering-parameters of a three-port device may be measured using a two-port VNA with the same technique [5]. Figure 4 illustrates such a setup, where the two-port VNA is connected to ports 1 and 3 of the divider, respectively.

In this configuration, b'_1 is a linear function of the signal reflected from port 1 of the divider and b'_3 is a linear function of the signal reflected from port 3. Thus, as in Eq. (3.2), the actual reflection coefficient is

$$\Gamma = \frac{b_2}{a_2} = \frac{(b'_1/b'_3) - e_{00}}{(b'_1/b'_3)e_{11} - \Delta_e} \quad (3.4)$$

or

$$\Gamma = \frac{b_2}{a_2} = \frac{\Gamma' - e_{00}}{\Gamma' \Gamma_G - \Delta_e}, \quad (3.5)$$

where

$$\Gamma' = b'_1/b'_3. \quad (3.6)$$

Equation (3.5) can be solved by connecting three devices with known values of reflection coefficients to port 2 of the divider, where Γ_G is the only term of interest, although e_{00} and Δ_e are also unknowns that can be determined.

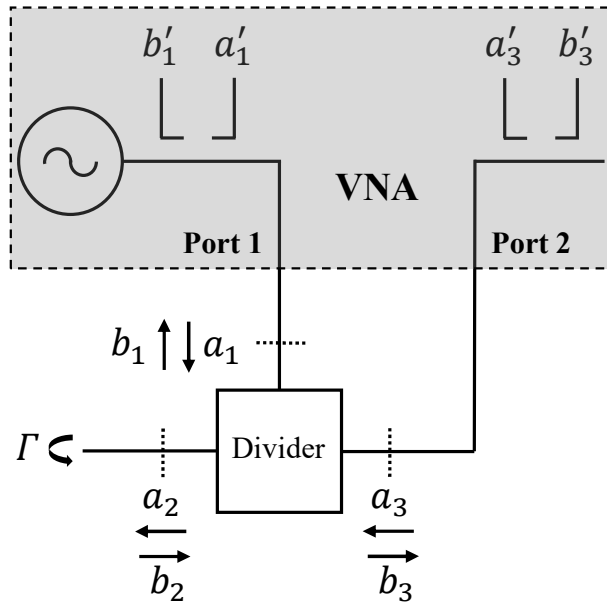


Fig. 4. Simplified diagram for measuring the equivalent source mismatch of a three-port device, such as a power divider, with a two-port VNA.

Juroshek [5] summarizes the take-away from this method as:

“It is important to realize that devices with loss and/or reflection can be connected to either port 1 or port 3 of the coupler [*in our case, divider*] without changing Γ_G assuming that the noise does not increase significantly due to the finite dynamic range of the VNA that measures b'_1 and b'_3 . For example, an adapter with reasonable losses and reflections can be connected to port 1 without changing Γ_G because the same change occurs in both S_{13} and S_{12} and, therefore, cancels out when the ratio is taken in Equation 3 [*in our case (2.25)*]. The same outcome is true for port 3. However, the outcome will be different for port 2 and any such connection will affect Γ_G directly. Thus, it is not important where b'_1 and b'_3 are measured as long as the dynamic range of the VNA is sufficient to measure them with the accuracy desired.”

3.2. Simplistic Derivation

In this section, we derive Eq. (3.5) and Eq. (2.25) using a simplistic model consisting of a three-port device, where ports 1 and 3 are well-matched such that Γ_1 and Γ_3 are zero, as shown in Fig. 5.

We begin with the scattering-matrix representation of a three-port device, which represents the divider:

$$\begin{bmatrix} b_1 \\ b_2 \\ b_3 \end{bmatrix} = \begin{bmatrix} S_{11} & S_{12} & S_{13} \\ S_{21} & S_{22} & S_{23} \\ S_{31} & S_{32} & S_{33} \end{bmatrix} \begin{bmatrix} a_1 \\ a_2 \\ a_3 \end{bmatrix}. \quad (3.7)$$

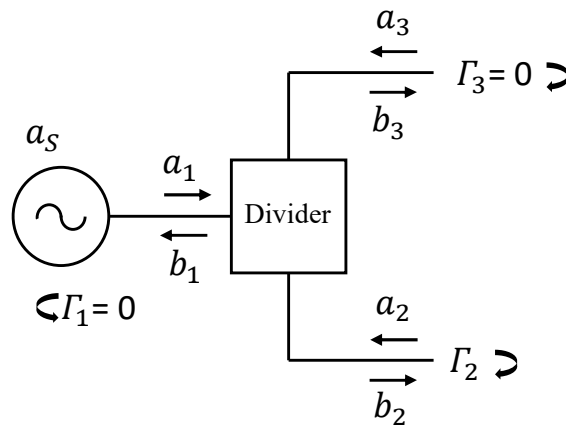


Fig. 5. Diagram a three-port device used in the simplistic derivation.

As in the previous section, our measured reflection coefficient is

$$\Gamma' = b_1/b_3. \quad (3.8)$$

Next, we assume the termination on port 3 is well-matched such that a_3 is equal to zero. From (3.7), we can extract the equations for the b waves:

$$b_1 = S_{11}a_1 + S_{12}a_2, \quad (3.9)$$

$$b_2 = S_{21}a_1 + S_{22}a_2, \quad (3.10)$$

and

$$b_3 = S_{31}a_1 + S_{32}a_2. \quad (3.11)$$

Solving Eq. (3.10) for Γ_2 gives

$$\Gamma_2 = \frac{a_2}{b_2} = \frac{a_2}{S_{21}a_1 + S_{22}a_2} = \frac{1}{S_{21}(a_1/a_2) + S_{22}}. \quad (3.12)$$

Taking the ratios of Eq. (3.9) and Eq. (3.11) gives Γ' :

$$\Gamma' = \frac{b_1}{b_3} = \frac{S_{11}a_1 + S_{12}a_2}{S_{31}a_1 + S_{32}a_2} \quad (3.13)$$

or

$$\Gamma' = \frac{S_{11}(a_1/a_2) + S_{12}}{S_{31}(a_1/a_2) + S_{32}}. \quad (3.14)$$

Multiplying both sides of Eq. (3.14) by the denominator of the right-hand side of the equation gives

$$S_{11}(a_1/a_2) + S_{12} = \Gamma' S_{31}(a_1/a_2) + \Gamma' S_{32}, \quad (3.15)$$

and solving for a_1/a_2 gives

$$\frac{a_1}{a_2} = \frac{\Gamma' S_{32} - S_{12}}{S_{11} - \Gamma' S_{31}}. \quad (3.16)$$

Substituting Eq. (3.16) into Eq. (3.12) gives

$$\Gamma_2 = \frac{1}{S_{21} \left(\frac{\Gamma' S_{32} - S_{12}}{S_{11} - \Gamma' S_{31}} \right) + S_{22}} \quad (3.17)$$

or

$$\Gamma_2 = \frac{\Gamma' - S_{11}/S_{31}}{\Gamma' \left(S_{22} - \frac{S_{21}S_{32}}{S_{31}} \right) - \frac{1}{S_{31}} (S_{11}S_{22} - S_{12}S_{21})}. \quad (3.18)$$

Equation (3.18) can be written as

$$\Gamma_2 = \frac{\Gamma' - e_{00}}{\Gamma' \Gamma_G - \Delta_e}, \quad (3.19)$$

where,

$$e_{00} = \frac{S_{11}}{S_{31}}, \quad (3.20)$$

$$\Delta_e = \frac{1}{S_{31}} (S_{11}S_{22} - S_{12}S_{21}), \quad (3.21)$$

and

$$\Gamma_G = S_{22} - \frac{S_{21}S_{32}}{S_{31}}. \quad (3.22)$$

Equation (3.19) is identical to Eq. (3.5), and Eq. (3.22) is the same as Eq. (2.25).

3.3. Comprehensive Derivation

In this section, we derive Eq. (3.5) and Eq. (2.25) using a comprehensive model consisting of a three-port device, as shown in Fig. 6, where we explicitly include the reflection coefficients at ports 1 and 3.

Here, we utilize matrix notation (shown in bold type) to help simplify the math. We begin by expressing the b -waves in terms of the scattering matrix of the divider multiplied by the a -waves:

$$\mathbf{b} = \mathbf{S}\mathbf{a}. \quad (3.23)$$

The a -waves can be expressed as functions of the reflection coefficients multiplied by the b -waves plus the contribution of the source:

$$\mathbf{a} = \mathbf{\Gamma}\mathbf{b} + \mathbf{a}_S. \quad (3.24)$$

Substituting Eq. (3.24) into Eq. (3.23) gives

$$\mathbf{b} = \mathbf{S}(\mathbf{\Gamma}\mathbf{b} + \mathbf{a}_S), \quad (3.25)$$

or

$$\mathbf{b} = \mathbf{S}\mathbf{\Gamma}\mathbf{b} + \mathbf{S}\mathbf{a}_S. \quad (3.26)$$

Solving for \mathbf{b} gives

$$\mathbf{b} = (\mathbf{I} - \mathbf{S}\mathbf{\Gamma})^{-1}\mathbf{S}\mathbf{a}_S, \quad (3.27)$$

where

$$\mathbf{a}_S = \begin{bmatrix} a_{S1} \\ 0 \\ 0 \end{bmatrix}. \quad (3.28)$$

The product $\mathbf{S}\mathbf{a}_S$ is

$$\mathbf{S}\mathbf{a}_S = \begin{bmatrix} S_{11} & S_{12} & S_{13} \\ S_{21} & S_{22} & S_{23} \\ S_{31} & S_{32} & S_{33} \end{bmatrix} \begin{bmatrix} a_{S1} \\ 0 \\ 0 \end{bmatrix} = \begin{bmatrix} S_{11}a_{S1} \\ S_{21}a_{S1} \\ S_{31}a_{S1} \end{bmatrix}, \quad (3.29)$$

and the product $\mathbf{S}\mathbf{\Gamma}$ is

$$\mathbf{S}\mathbf{\Gamma} = \begin{bmatrix} S_{11} & S_{12} & S_{13} \\ S_{21} & S_{22} & S_{23} \\ S_{31} & S_{32} & S_{33} \end{bmatrix} \begin{bmatrix} \Gamma_1 & 0 & 0 \\ 0 & \Gamma_2 & 0 \\ 0 & 0 & \Gamma_3 \end{bmatrix} = \begin{bmatrix} \Gamma_1 S_{11} & \Gamma_2 S_{12} & \Gamma_3 S_{13} \\ \Gamma_1 S_{21} & \Gamma_2 S_{22} & \Gamma_3 S_{23} \\ \Gamma_1 S_{31} & \Gamma_2 S_{32} & \Gamma_3 S_{33} \end{bmatrix}, \quad (3.30)$$

where the off-diagonal elements of the $\mathbf{\Gamma}$ matrix are zero since there are no cross-port reflections.

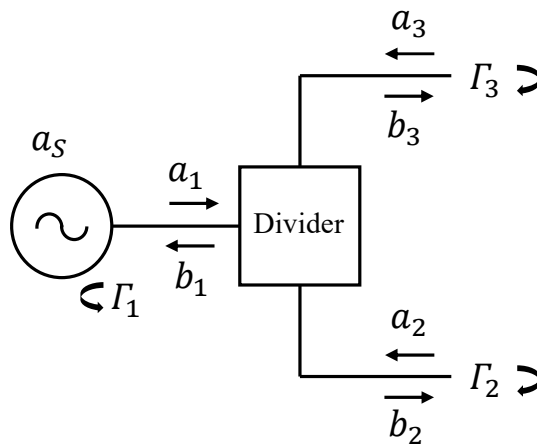


Fig. 6. Diagram a three-port device used in the comprehensive derivation.

The term $I - SF$ is

$$I - SF = \begin{bmatrix} 1 - \Gamma_1 S_{11} & -\Gamma_2 S_{12} & -\Gamma_3 S_{13} \\ -\Gamma_1 S_{21} & 1 - \Gamma_2 S_{22} & -\Gamma_3 S_{23} \\ -\Gamma_1 S_{31} & -\Gamma_2 S_{32} & 1 - \Gamma_3 S_{33} \end{bmatrix}. \quad (3.31)$$

Substituting Eq. (3.29) and Eq. (3.31) into Eq. (3.27) gives

$$\begin{bmatrix} b_1 \\ b_2 \\ b_3 \end{bmatrix} = \begin{bmatrix} 1 - \Gamma_1 S_{11} & -\Gamma_2 S_{12} & -\Gamma_3 S_{13} \\ -\Gamma_1 S_{21} & 1 - \Gamma_2 S_{22} & -\Gamma_3 S_{23} \\ -\Gamma_1 S_{31} & -\Gamma_2 S_{32} & 1 - \Gamma_3 S_{33} \end{bmatrix}^{-1} \begin{bmatrix} S_{11} a_{S1} \\ S_{21} a_{S1} \\ S_{31} a_{S1} \end{bmatrix}, \quad (3.32)$$

where we define A as

$$A = \begin{bmatrix} 1 - \Gamma_1 S_{11} & -\Gamma_2 S_{12} & -\Gamma_3 S_{13} \\ -\Gamma_1 S_{21} & 1 - \Gamma_2 S_{22} & -\Gamma_3 S_{23} \\ -\Gamma_1 S_{31} & -\Gamma_2 S_{32} & 1 - \Gamma_3 S_{33} \end{bmatrix}. \quad (3.33)$$

We can determine the following cofactors of A as

$$\text{cof}(A_{11}) = (1 - \Gamma_2 S_{22})(1 - \Gamma_3 S_{33}) - \Gamma_2 \Gamma_3 S_{23} S_{32}, \quad (3.34)$$

$$\text{cof}(A_{21}) = \Gamma_2 S_{12}(1 - \Gamma_3 S_{33}) + \Gamma_2 \Gamma_3 S_{13} S_{32}, \quad (3.35)$$

$$\text{cof}(A_{31}) = \Gamma_2 \Gamma_3 S_{12} S_{23} + \Gamma_3 S_{13}(1 - \Gamma_2 S_{22}), \quad (3.36)$$

$$\text{cof}(A_{13}) = \Gamma_1 \Gamma_2 S_{21} S_{32} + \Gamma_1 S_{31}(1 - \Gamma_2 S_{22}), \quad (3.37)$$

$$\text{cof}(A_{23}) = \Gamma_2 S_{32}(1 - \Gamma_1 S_{11}) + \Gamma_1 \Gamma_2 S_{12} S_{31}, \quad (3.38)$$

and

$$\text{cof}(A_{33}) = (1 - \Gamma_1 S_{11})(1 - \Gamma_2 S_{22}) - \Gamma_1 \Gamma_2 S_{12} S_{21}. \quad (3.39)$$

The terms b_1 and b_3 in Eq. (3.32) can then be extracted as

$$b_1 = \frac{1}{\det(A)} [S_{11} \text{cof}(A_{11}) + S_{21} \text{cof}(A_{21}) + S_{31} \text{cof}(A_{31})] a_{S1} \quad (3.40)$$

and

$$b_3 = \frac{1}{\det(A)} [S_{11} \text{cof}(A_{13}) + S_{21} \text{cof}(A_{23}) + S_{31} \text{cof}(A_{33})] a_{S1}. \quad (3.41)$$

The measured reflection coefficient Γ' is the ratio of b_1 and b_3 :

$$\Gamma' = \frac{b_1}{b_3} = \frac{S_{11}\text{cof}(A_{11}) + S_{21}\text{cof}(A_{21}) + S_{31}\text{cof}(A_{31})}{S_{11}\text{cof}(A_{13}) + S_{21}\text{cof}(A_{23}) + S_{31}\text{cof}(A_{33})}. \quad (3.42)$$

Substituting Eqs. (3.34-3.39) into Eq. (3.42) gives

$$\Gamma' = \frac{\left\{ \begin{array}{l} S_{11}[(1 - \Gamma_2 S_{22})(1 - \Gamma_3 S_{33}) - \Gamma_2 \Gamma_3 S_{23} S_{32}] \\ + S_{21}[\Gamma_2 S_{12}(1 - \Gamma_3 S_{33}) + \Gamma_2 \Gamma_3 S_{13} S_{32}] \\ + S_{31}[\Gamma_2 \Gamma_3 S_{12} S_{23} + \Gamma_3 S_{13}(1 - \Gamma_2 S_{22})] \end{array} \right\}}{\left\{ \begin{array}{l} S_{11}[\Gamma_1 \Gamma_2 S_{21} S_{32} + \Gamma_1 S_{31}(1 - \Gamma_2 S_{22})] \\ + S_{21}[\Gamma_2 S_{32}(1 - \Gamma_1 S_{11}) + \Gamma_1 \Gamma_2 S_{12} S_{31}] \\ + S_{31}[(1 - \Gamma_1 S_{11})(1 - \Gamma_2 S_{22}) - \Gamma_1 \Gamma_2 S_{12} S_{21}] \end{array} \right\}}. \quad (3.43)$$

Equation (3.43) can be expressed as

$$\Gamma' = \frac{\alpha \Gamma_2 + \beta}{\gamma \Gamma_2 + \theta}, \quad (3.44)$$

where

$$\alpha = (S_{12} S_{21} - S_{11} S_{22}) + \Gamma_3 \left(\begin{array}{l} S_{11} S_{22} S_{33} - S_{11} S_{23} S_{32} - S_{12} S_{21} S_{33} \\ + S_{12} S_{23} S_{31} + S_{13} S_{21} S_{32} - S_{13} S_{22} S_{31} \end{array} \right), \quad (3.45)$$

$$\beta = S_{11} + \Gamma_3 (S_{13} S_{31} - S_{11} S_{33}), \quad (3.46)$$

$$\gamma = S_{21} S_{32} - S_{22} S_{31}, \quad (3.47)$$

and

$$\theta = S_{31}. \quad (3.48)$$

Equation (3.44) can be rearranged as

$$\Gamma_2 = \frac{\Gamma' - \left(\frac{\beta}{\theta}\right)}{\Gamma' \left(-\frac{\gamma}{\theta}\right) - \left(\frac{\alpha}{\theta}\right)}. \quad (3.49)$$

Comparing Eq. (3.49) with Eq. (3.19), we see that the equivalent source mismatch term Γ_G is

$$\Gamma_G = -\frac{\gamma}{\theta}. \quad (3.50)$$

Substituting Eq. (3.47) and Eq. (3.48) into Eq. (3.50) gives

$$\Gamma_G = -\frac{S_{21} S_{32} - S_{22} S_{31}}{S_{31}}, \quad (3.51)$$

or

$$\Gamma_G = S_{22} - \frac{S_{21}S_{32}}{S_{31}}. \quad (3.52)$$

Equation (3.52) is identical to Eq. (3.22). From this comprehensive derivation, we can see that Γ_G is independent of Γ_1 and Γ_3 . This result is consistent with Juroshek's conclusion [5].

4. Conclusions

We have provided derivations for the equations that govern the direct-comparison system utilizing scattering-parameter flow diagrams and power definitions. Additionally, we specified a correction term for the case when an adapter is connected to the known power sensor. Finally, we reviewed the most widely-accepted approach for determining the equivalent source reflection coefficient of a three-port device, such as a power divider, and provided derivations that demonstrate its independence of external impedance mismatches at two of its ports.

Acknowledgments

The authors thank Jim Booth, Ari Feldman, Paul Hale, Mitch Wallis, and Dylan Williams for their helpful comments.

References

- [1] Clague FR, Voris PG (1993) Coaxial reference standard for microwave power (National Institute of Standards and Technology, Boulder, CO), NIST Technical Note (TN)1357.
- [2] Weidman MP (1996) Direct comparison transfer of microwave power sensor calibrations (National Institute of Standards and Technology, Boulder, CO), NIST Technical Note (TN) 1379.
- [3] Juroshek JR (2000) NIST 0.05-50 GHz direct-comparison power calibration system. *Conference on Precision Electromagnetic Measurements*, pp. 166-167.
- [4] Rytting D (1987) Advances in microwave error correction techniques. *RF and Microwave Measurement Symposium*.
- [5] Juroshek JR (1997) A direct calibration method for measuring equivalent source mismatch. *Microwave Journal*, pp. 106–118.
- [6] Kerns DM, Beatty RW (1967) Basic Theory of Waveguide Junctions and Introductory Microwave Network Analysis (Pergamon Press).
- [7] Keysight Technologies (2104) Fundamentals of RF and Microwave Power Measurements (Part 3). Application Note 1449-3, 5988-9215EN.
- [8] Teppati V, Ferrero A, Sayed M (2013) Modern RF and Microwave Measurement Techniques (Cambridge University Press).
- [9] Engen GF (1958) Amplitude stabilization of a microwave signal source. *IRE Transactions on Microwave Theory and Techniques*, 6(2): 202-206.
- [10] Fantom A (1990) Radio Frequency and Microwave Power Measurement (Peter Peregrinus).

- [11] Wallis TM, Crowley TP, LeGolvan DX, Ginley RA (2012) A direct comparison system for power calibration up to 67 GHz. *Conference on Precision Electromagnetic Measurements*, pp. 726-727.
- [12] Kang TW, Kim JH, Kwon JY, Park JI, Lee DJ (2012) Direct comparison technique using a transfer power standard with an adapter and its uncertainty. *Conference on Precision Electromagnetic Measurements*, pp. 728-729.